Digest Journal of Nanomaterials and Biostructures Vol. 16, No. 4, October-December 2021, p. 1411-1425

Reaction mechanism comparison of AlSi-polyester and aluminum bronze/polyester plasma spraying

C. Ju[a], Q. Li[b], Z. L. Wang[a], Q. H.Song[a], J. J. Li[a], Z. P. Sun[a], Y. F. Zhang[a,*]
[a]*School of Mechanical & Automotive Engineering, Qilu University of Technology (Shandong Academy of Sciences), Jinan, Shandong, 250353, PR China*
[b]*School of Material Science & Engineering, Qilu University of Technology (Shandong Academy of Sciences), Jinan, Shandong, 250353, PR China*

AlSi-polyester seal coatings and aluminum bronze/polyester seal coatings prepared by plasma spraying were used to study their reaction mechanism. The composition of AlSi-polylester and aluminum bronze/polyester powders and coatings were investigated by X-ray diffraction. The powders were analyzed by thermogravimetric differential thermal analysis and scanning electron microscopy. Comparing the powder with the coating, it is found that they have the same phase by X-ray diffraction. Thermogravimetric differential thermal analysis of the powders show that the service temperature should not exceed 500^{o}C, otherwise the polyester constituent begins to degrade. It is also found that the aluminum bronze/polyester seal coatings have a lower porosity than the AlSi-polyester seal coatings.

(Received July 17, 2021; Accepted November 7, 2021)

Keywords: AlSi-polyester, Aluminum bronze/polyester, Plasma spraying, Seal coatings, Phase

1. Introduction

Seal coatings have been widely used on aircraft engines to provide clearance control for the casing and blades of aircraft engines and turbines, which can significantly improve engine efficiency and save fuel [1]. Therefore, the seal coatings must have the following properties: abrasion resistance, erosion resistance, strong bonding strength, thermal shock resistance, low coefficient of friction and anti-adhesion, high chemical stability and overall strength, etc. The seal coatings usually consists of three parts: a metal matrix, a non-metallic lubricant, and some pores [2-4]. In recent years, as the research on seal coatings have become more intensive, the spraying process becomes more and more mature, the aluminum bronze/polyester powder and the AlSi-polyester powder developed by Metco are widely used [5-7]. More research has focused on the composition and distribution of the abradable phase after coating application. As for the phase change and surface morphology after thermal spraying, there are few analysis. In fact, the study of the changes after thermal spraying allows for a better understanding of the reaction mechanism

* Corresponding author: zhangyanfei@qlu.edu.cn

of the spraying process and thus the discovery of optimal parameters [8-13]. Researchers have investigated the content and distribution of the polyester phase of AlSi-polyester seal coatings, they found when the content of polyester is similar, the more uniform the distribution of the polyester phase, the smaller the particles and the smaller the friction coefficient [0].

2. Material and methods

2.1. Materials

The AlSi-polyester powders (Metco 601NS) and aluminum bronze/polyester powders (Metco 604NS) are supplied by Oerlikon Metco (Winterthur, Switzerland). Metco 601NS composite powder has a particle size of -125±11μm and a composition ratio of 60% AlSi + 40% polyester. Metco 604NS has a particle size of -125±11μm and a composition ratio of 95% aluminum bronze + 5% polyester.

2.2. Experimental procedure

All the seal coatings were sprayed by atmospheric plasma sprayed (APS) process. Before spraying, the surface of annealed 45 steel (HRC22 ~ 25) were cleaned by acetone and then sand blasted with corundum grits. Metco 604NS powders were sprayed directly onto the processed substrate. As for Metco 601NS, bond coat was plasma sprayed with commercial Metco 404NS powders from Oerlikon Metco. Afterwards, Metco 601NS powders were deposited onto the surfaces of the bond coat using the APS process. Table 1 shows the parameters used.

Table 1. Spray parameters for the APS process.

Powder	Metco 604NS	Metco 601NS	Metco 404NS
Current (A)	500	495	495
Voltage (V)	55	68	68
Primary gas (Ar, PSI)	75	75	75
Secondary gas (H_2, PSI)	50	50	50
Argon flow rate (SCFH)	160	180	90
Powder feed air flow rate (NLPM)	6	9	8
Spray distance (mm)	110	105	105

Thermogravimetric differential thermal analysis (TG-DTA) of powder was performed on a STA 449F3 synchronous thermal analyzer (NETZSCH, Germany). The X-ray diffraction (XRD) patterns of the samples were obtained on D8-ADVANCE (AXS, Germany). The morphologies and microstructures of the powders and coatings were evaluated by scanning electron microscopy (SEM, GeminiSEM 500, Carl Zeiss, Germany). The powders and coatings were impregnated with epoxy. After hardening of the resin, the sample was ground with SiC abrasive paper and polished on soft disks with diamond suspension. A cross section of the sample was investigated by SEM and Digital Microscope VHX-5000 (KEYENCE, Japan).

3. Results and discussion

3.1 Powders surface and composition

3.1.1 Metco 601NS

Figure 1 shows the surface morphologies of the AlSi-polyester composite powders. The AlSi-polyester composite powders are irregularly agglomerated. They exhibit two different morphologies, marked as A and B in Figure 1c and Figure 1d. According to the results of energy dispersive spectrometer (EDS) , region A is mainly composed of C, Al and Si, so region A can be determined to be Al and Si. Region B is basically composed of C, N and O, indicating that the powder is polyester phase [0]. According to EDS element mapping results (Figure 1e), it can be concluded that the agglomerated particles are polyester, and the spherical particles with smooth surface are AlSi alloy. Most polyester particles are larger than AlSi alloy particles, and a small amount of small AlSi alloy particles adhere to the surface of polyester particles.

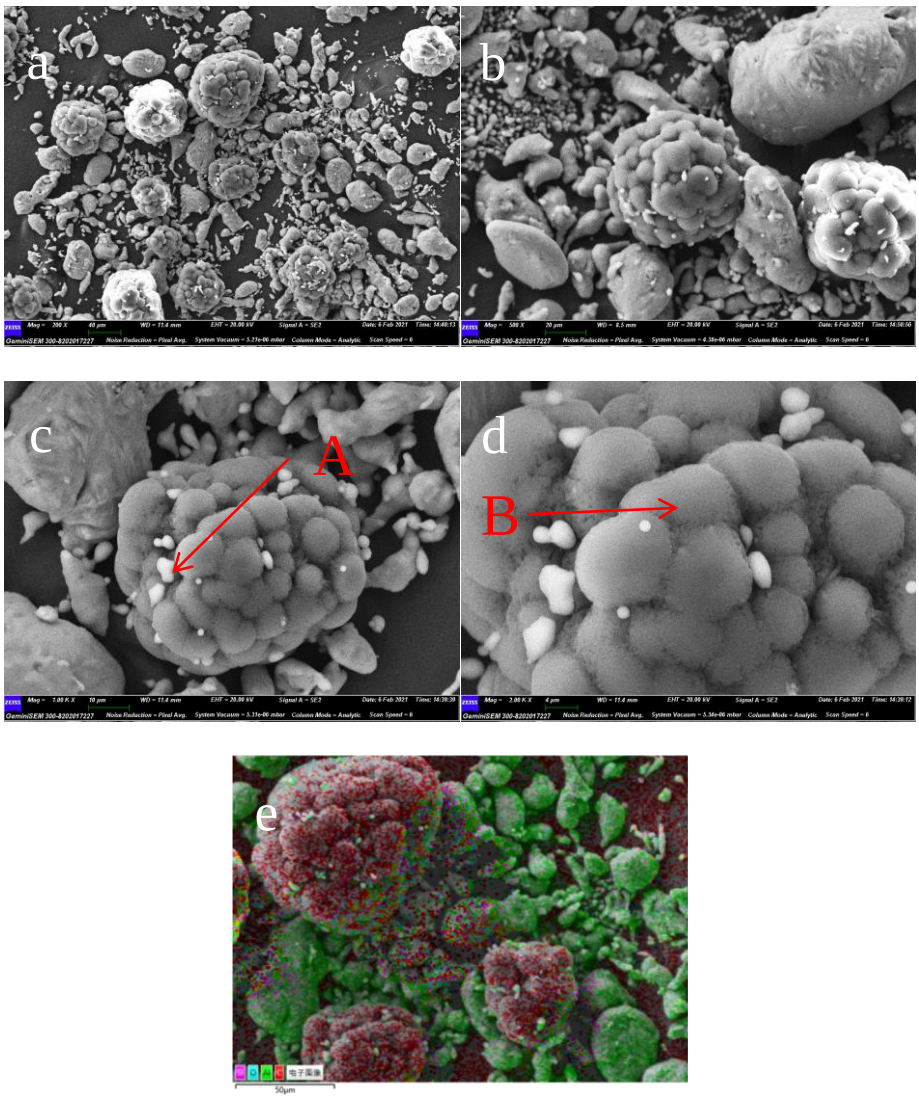

Fig. 1. The surface morphology of AlSi-polyester composite powders and the EDS element mapping.

AlSi-polyester powders were manufactured by blending AlSi alloy powders and polyester powders. And composite structure facilitates the plasma spraying process and reduces the burnout of the polyester. Due to the high viscosity of the polyester powder, the aggregated AlSi-polyester powder cannot flow down autonomously without external pushing [0].

Cross section of AlSi-polyester composite powder is shown in Figure 2. Region A is AlSi alloy while region B is agglomerated polyester. It can be seen that part of AlSi alloys are adhered around the agglomerated polyester. And agglomerated polyester shows a regular round shape.

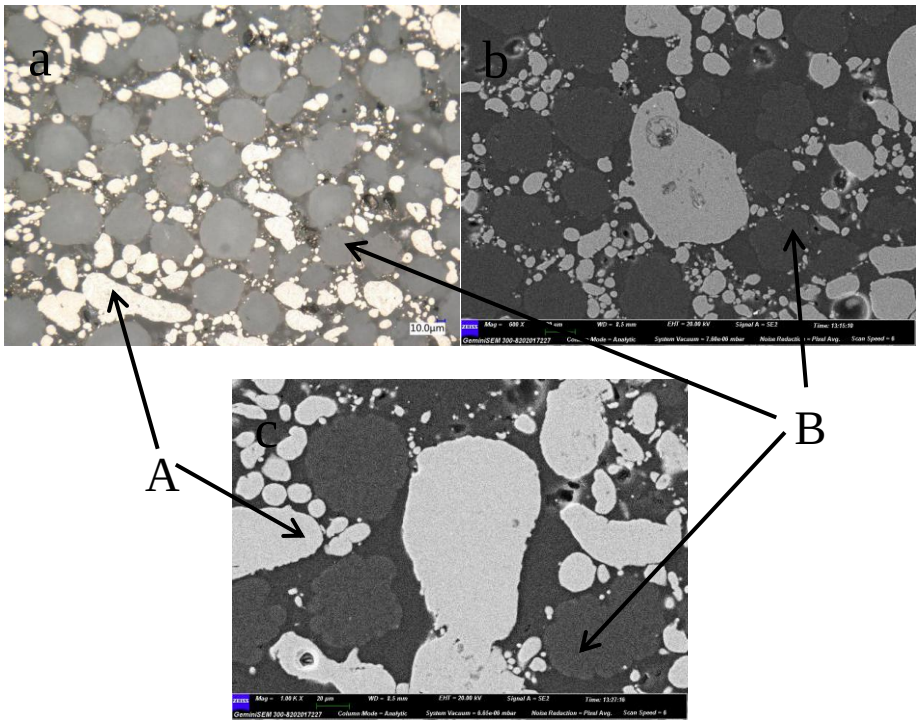

Fig. 2. Cross section of AlSi-polyester composite powders.

3.1.2. Metco 604NS

The surface morphologies of aluminum bronze/polyester composite powders are shown in Figure 3. It is evident that the powder is composed of two phases, one spherical and one agglomerated.

According to the results of EDS, region A is mainly comprised of Al, Fe and Cu, and N element does not exist, so region A can be determined to be aluminum bronze phase. Region B is basically composed of C, N and O, Al element does not exist, indicating that the powder is polyester phase. It can be inferred that the agglomerates are polyesters, which are prepared as "lubricating components" after spraying [17-18]. According to Figure 3e, it can be seen that the agglomerate particle is polyester and the spherical particle is aluminum bronze. A small amount of aluminum bronze alloys are adhered on the surface of the polyester. The particle size of polyester is larger than that of aluminum bronze alloy.

So the aluminum bronze/polyester powders are made of two kinds of materials, namely polyester powders and aluminum bronze powders, mixed using blending method.

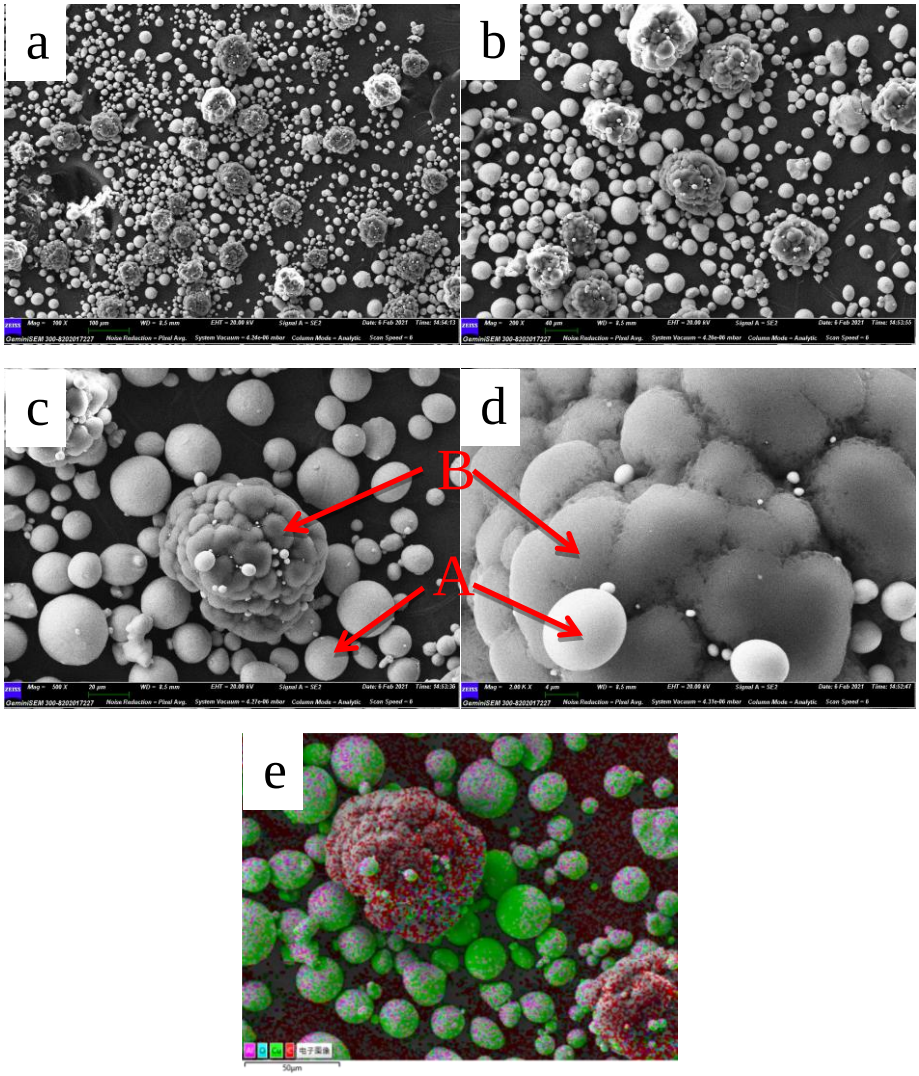

Fig. 3. The surface morphology of aluminum bronze/polyester composite powders and EDS element mapping.

Comparing AlSi-polyester powders and aluminum bronze/polyester powders, it can be concluded that both of the powders are prepared by blending method, and some alloys are adhered to the polyester, and the polyester particles are larger than most alloy particles. The difference between the two powders is that aluminum bronze is the spherical, while AlSi alloy is irregular in shape. So Metco 604NS powders have less polyester and better flowability than Metco 601NS.

3.2. Surface morphology and composition of the coating

3.2.1. Metco 601NS coating

Figure 4 shows the surface morphologies of the AlSi-polyester coating after plasma spraying. The AlSi-polyester coating is a composite coating with the polyester region and the AlSi alloy region present in the coating. The powder had partially unmelted in some areas. The

combination between AlSi and polyester is tight, there are evenly distributed between each other with relatively low porosity and no cracks [0].

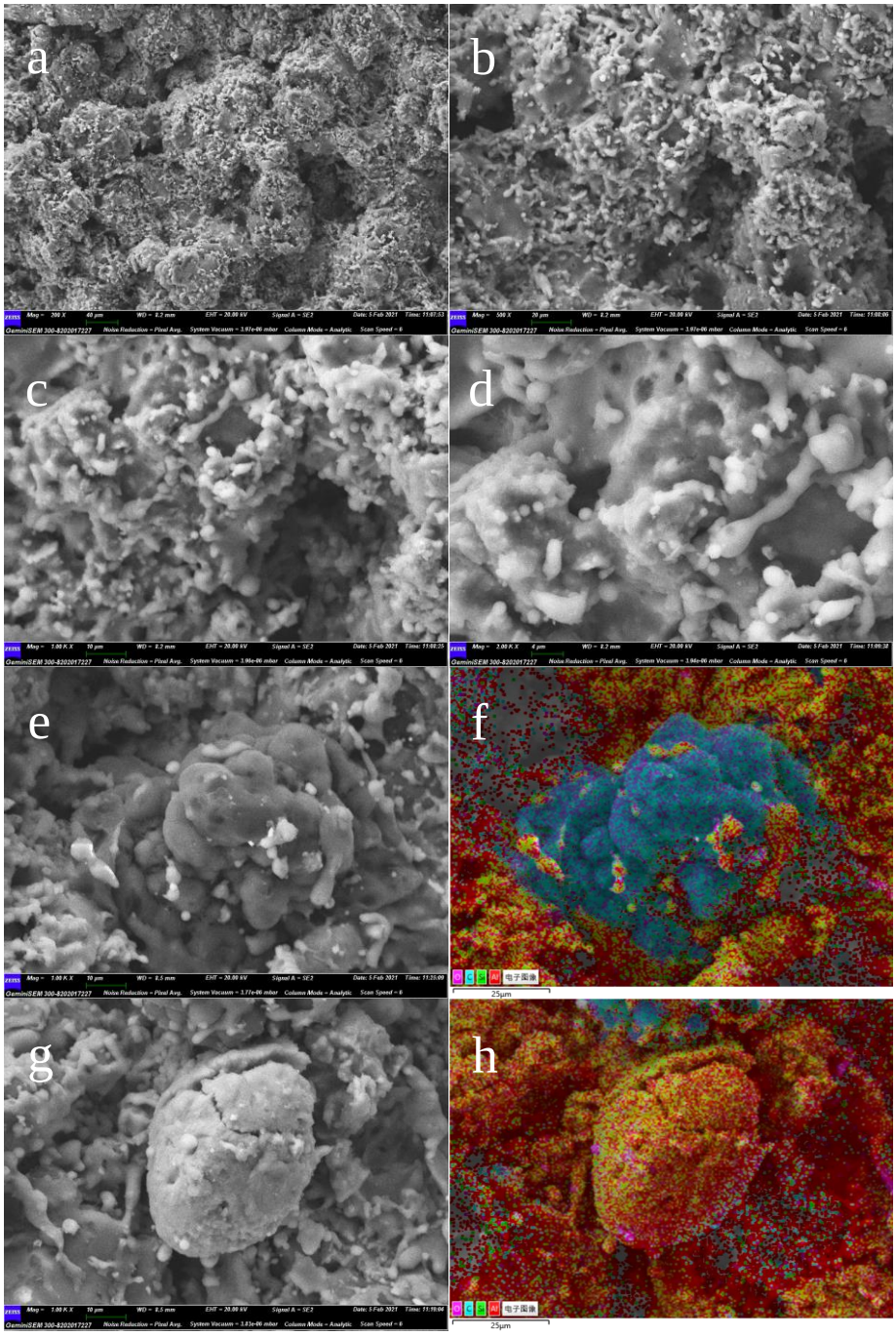

Fig. 4. SEM morphology of AlSi-polyester coating and the EDS element mapping.

Figure 4 shows corresponding EDS element mapping of AlSi-polyester coating. The elements contained in the coating are basically Si, Al, C and O. Powder and coating compositions basically stay consistent. Figure 4e-h show unmelted polyesters and AlSi alloys powders during plasma spraying. O is observed on the AlSi alloys powders surface, which indicates the oxidation of alloys during plasma spraying.

Figure 5 shows cross-section of the Metco 601NS coating, and it is clear that the coating is divided into two layers, the upper layer being Metco 601NS seal coating, the lower layer being the bond coat prepared with Metco 404NS. Polyesters are evenly distributed with AlSi, and no cracks are found in the coating. As shown in Figure 5a-b, the grey region in the AlSi-polyester coating is the AlSi phase and the black region is the polyester phase [20-21]. The AlSi phase in the coating acts as the skeleton, giving the coating itself good strength and good bond strength with the substrate, making it have certain corrosion and thermal shock resistance. The main role of the polyester phase is to create pores during the spraying process, thereby reducing the hardness of the coating and improving the wear resistance of the coating. The AlSi-polyester coating is tightly bonded to the bond coat, with no pores or inclusions on the bond surface, and the coating structure is essentially uniform from outside to inside [22]. There is no separation or spalling between the coating and the bond coat, or between the bond coat and the substrate.

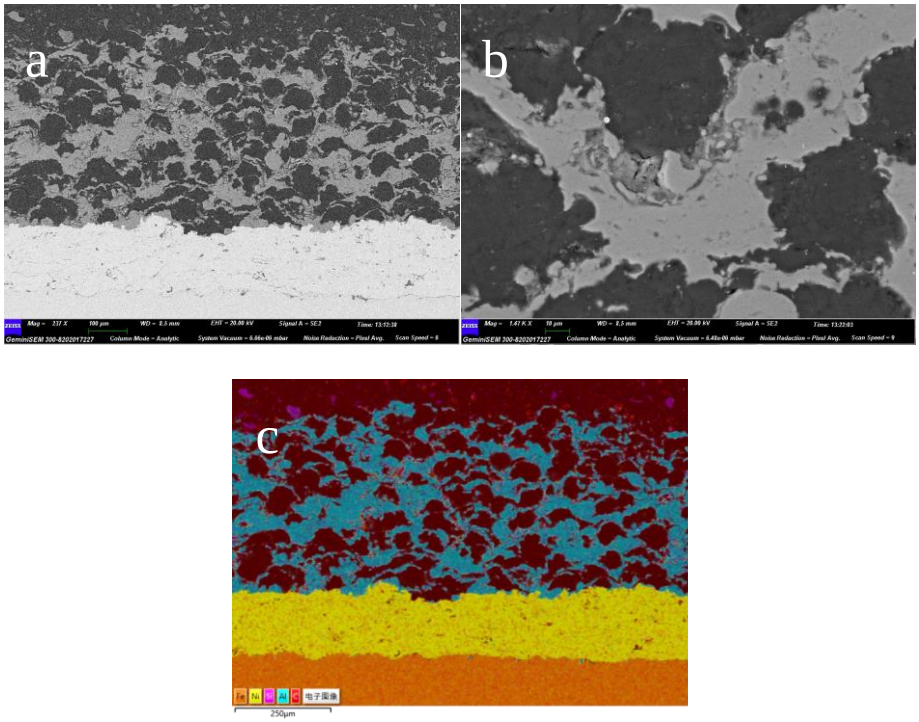

Fig. 5. SEM of AlSi-polyester coating cross section (a) and the corresponding EDS element mapping.

3.2.2. Metco 604NS coating

Figure 6 shows the surface morphology of the aluminum bronze/polyester coating after plasma spraying. The reason for this morphology is the unmelted and partially melted state of the particles impacting on the surface of the substrate material at high speed under the action of spray jet. Due to the high kinetic energy, the particles rapidly spread on the surface of the substrate material and solidify to form lamellar sheets. The subsequent particles continue to impact on the surface of the substrate material at high speed, resulting in plastic deformation. And the compacting effect formed by the undeposited particles on the deposited particles is beneficial to increase the coating density. However, there are still a small number of unmelted or partially melted particles, gaps between flat particles stacked on top of each other, and holes where some

particles join each other in Figure 6. It can be seen from the EDS element mapping that both polyester particles and aluminum bronze particles have unmelted particles (Figure 6f-g).

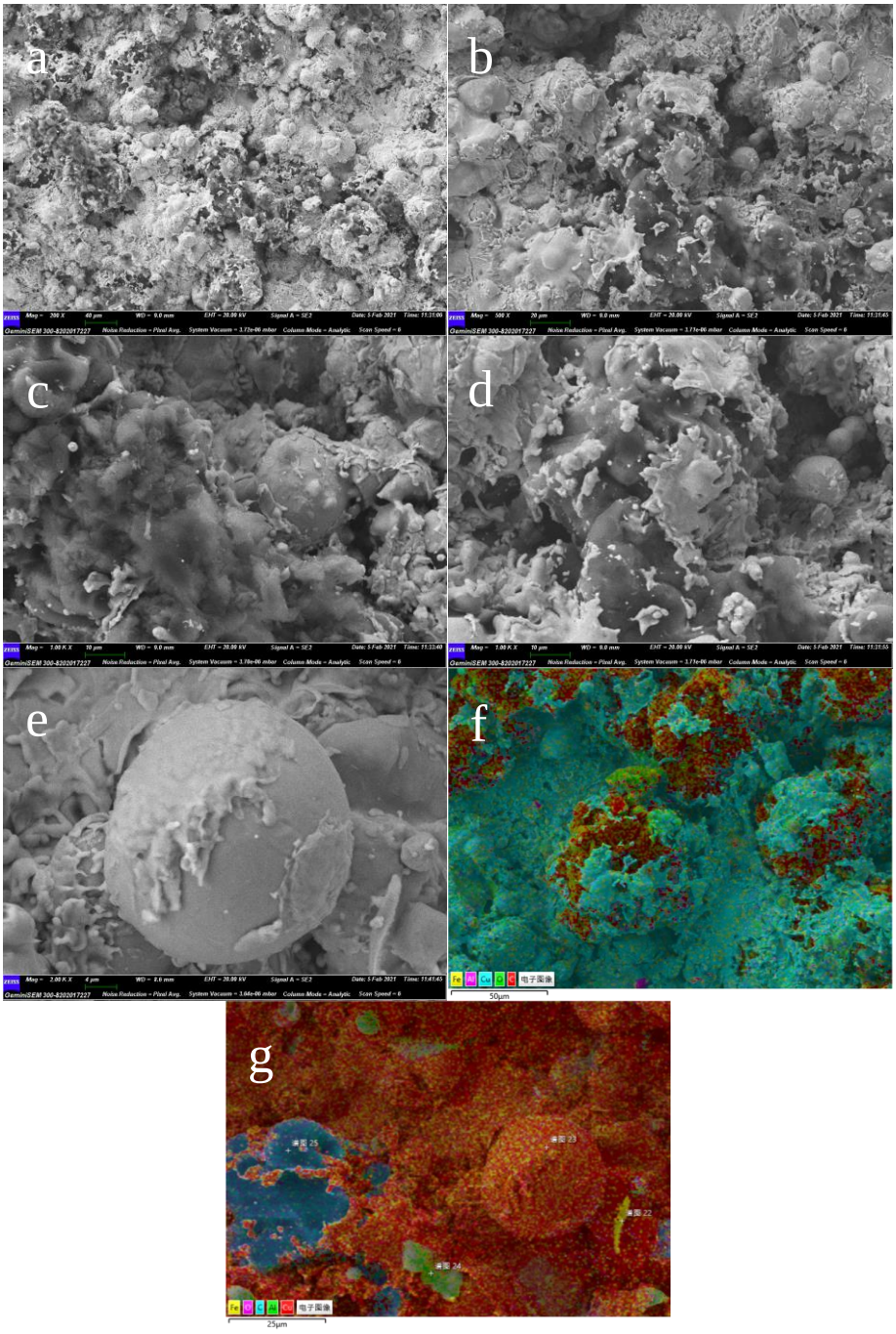

Fig. 6. SEM morphology of the aluminum bronze/polyester coating surface and the corresponding EDS element mapping.

Figure 7 shows the electron backscattered diffraction (EBSD) of aluminum bronze/polyester coating. EBSD is a technique for determining crystal orientation, composition, etc. It works based on the analysis of the diffraction daisy-bands formed by electron beam excitation on the surface of a specimen in a scanning electron microscope. EBSD analysis has many advantages, such as speed, quantification, non-destructive, etc. In addition, it allows for

simultaneous analysis of elements. Generally, the heavy element areas such as the metallic phase areas are brighter and the lighter elements such as the non-metallic phase areas are darker in the EBSD images. So the white area is aluminum bronze and the black area is polyester in Figure 7.

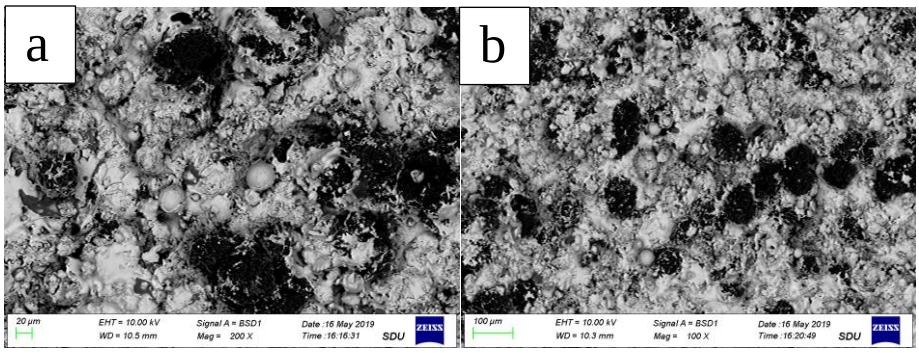

Fig. 7. The electron backscattered diffraction of aluminum bronze/polyester coating.

Table 2. Chemical compositions of region in Figure 8a.

Element	CK	OK	AlK	FeK	CuK
Wt%	7.23	1.37	43.05	31.82	16.53
At%	19.34	2.76	51.25	18.30	8.35

Table 3. Chemical compositions of region in Figure 8b.

Element	CK	OK	AlK	FeK	CuK
Wt%	13.39	6.66	48.30	21.03	4.33
At%	28.84	10.77	46.32	9.74	10.63

Table 4. Chemical compositions of region in Figure 8c.

Element	CK	OK	AlK	FeK	CuK
Wt%	64.23	15.72	4.75	3.40	11.89
At%	79.17	14.55	2.61	0.90	2.77

Table 2-4 is the EDS analysis of the coating surface in Figure 8. And it can be seen that the main elements of the lump in the coating in Figure 8c are C and O, which can be identified as polyesters. And the main elements contained in the smooth zone in Figure 8a are Al, Cu, Fe, etc, which should be the structure formed after the melting of aluminum bronze particles. The elements in the spherical region in Figure 8b are basically similar to those in the completely melted region in Figure 8a, which should be unmelted aluminum bronze particles. However, the EDS results in Figure 8a and Figure 8b show that the mass percentage of Cu is smaller than that of Al and Fe, which is at variance with other studies in the literature [0], which suggest that Cu should be the dominant element in aluminum bronze/polyester coatings.

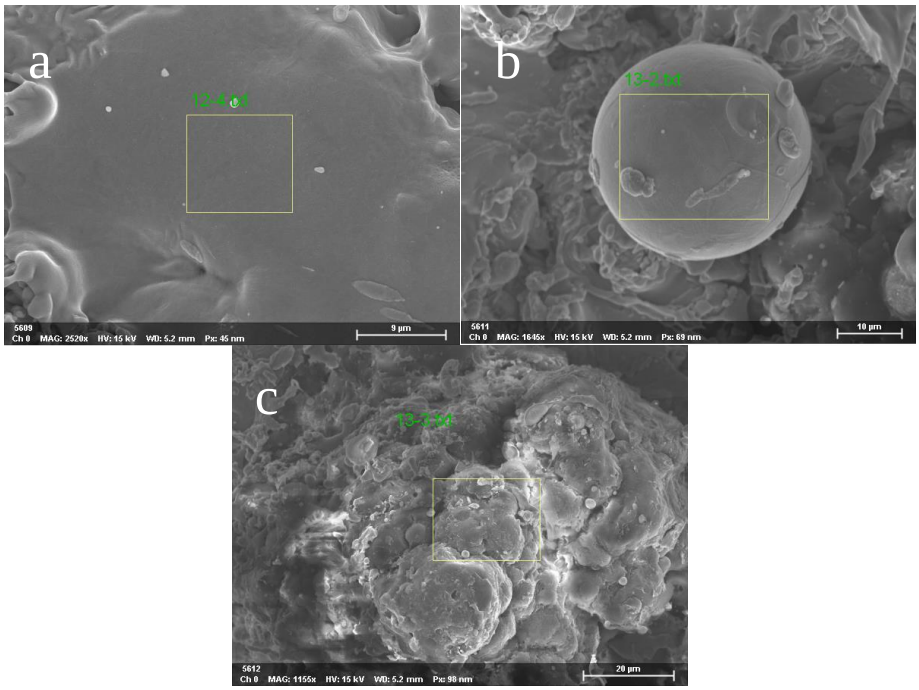

Fig. 8. EDS analysis of aluminum bronze/polyester coating surface morphology: (a) coating smooth zone, (b) coating spherical zone, (c) coating mass zone.

Figure 9a shows the cross-section of the coating, where the black areas are polyesters and the grey areas are aluminum bronze. The polyester is agglomerated, uniformly distributed in the coating, without obvious pores. There are microcracks at the junction of the coating and the substrate, which may be caused by residual stress.

As can be seen from the EDS element mapping in Figure 9, the elements contained in the coating are basically Cu, Al, Fe, C and O. Fe distribution in the coating is relatively uniform, with no significant bias. C and O are mainly concentrated in the black area in Figure 10a, so the black area in Figure 10a should be polyester. Cu are mainly concentrated in the grey area in Figure 9a, and evenly distributed in the grey area in Figure 9a, Al are mainly distributed in the grey area in Figure 9a. Therefore, the grey area in Figure 9a should be aluminum bronze. There was also a trace and basically uniform oxygen distribution in the coating, which indicates that aluminum bronze is oxided during plasma spraying.

In the plasma spraying process, the flame does not directly heat the substrate, and the melted or partially melted powder particles hit the surface of the substrate, and the cooling rate is fast. Therefore, excessive separation of elements in plasma sprayed coatings is avoided. The distribution of elements is relatively uniform. Although the powder is protected by protective gas during spraying, it still inevitably comes into contact with the atmosphere, so a trace of oxides will appear in the coating.

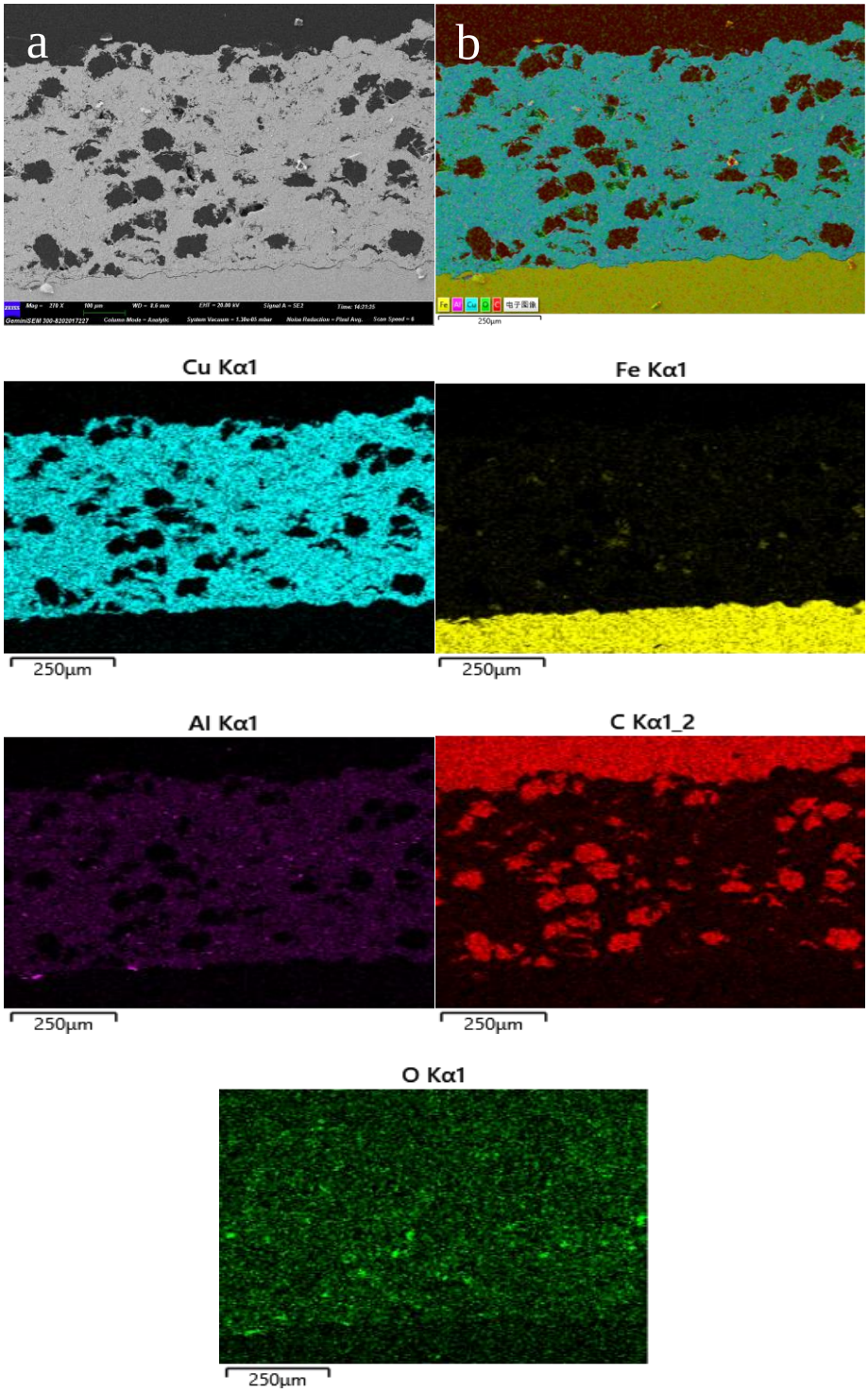

Fig. 9. SEM images of aluminum bronze/polyester coating cross-section and the corresponding EDS element mapping.

By comparing Metco 601NS with Metco 604NS coatings, it is found that they all need plasma spraying process. However, the bond coat is required before spraying the AlSi-polyester coating because high polyester percentage (40%) leads to decreased bonding strength with the substrate. At the same time, the seal coating keeps good bonding with the substrate, and no

separation or spalling occurs. The bonding of the coating to the substrate was mechanical. Pores were present in all the coatings, but the pores in Metco 601NS coatings were larger due to oxidation of the alloy and thermal decomposition of polyester. Coating prepared with Metco 604NS is denser due to lower polyester percentage (5%) and better melting effect of spherical aluminum bronze powders.

3.3. X-ray diffraction analysis

3.3.1. Metco 601NS

Figure 10 shows the XRD pattern of Metco 601NS coating and powder, as well as the standard card of Aluminum (PDF#04-0787) as a reference. The XRD result in Figure 10 shows that coating and powder mainly consisted of Al, Si and polyester. The phase of coating and powder are basically the same. The diffraction peaks decrease in intensity after spraying due to decreased crystallinity. No other new compounds were found after spraying, indicating that the structure of the AlSi-polyester is stable.

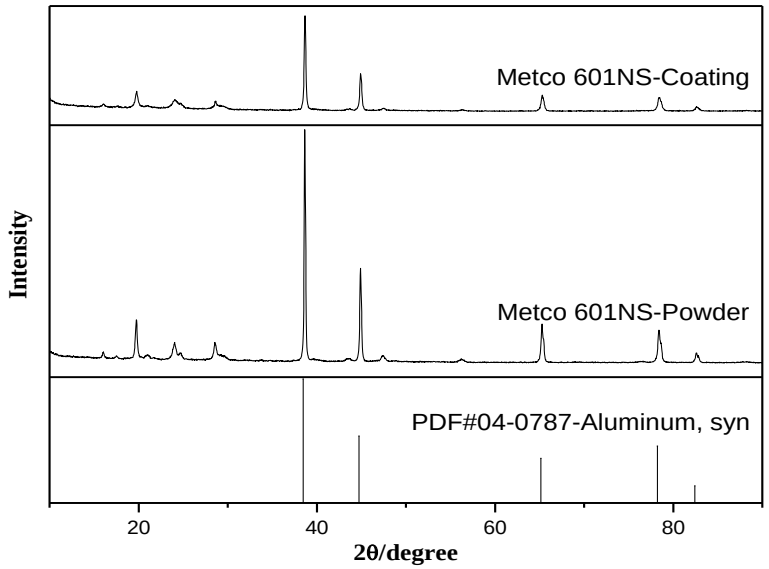

Fig. 10. XRD pattern of the AlSi-polyester coating and powder.

3.3.2. Metco 604NS

Figure 11 shows the XRD pattern of Metco 604NS coating and powder, as well as the standard card of $AlCu_3$ (PDF#28-0005) as a reference. The XRD result shows that the powder and coating compositions are essentially the same, indicating that the coatings prepared by the plasma spraying process have a greater retention of the excellent properties of the powder.

The main metal phase compositions of coatings and powders are α phase, β′ phase and Fe-containing K phase. α phase is a copper-based solid solution, and it is also the basic composition of the coating phase. It belongs to the face-centered cubic structure and has good mechanical properties, plastic deformation ability and low hardness. β′ phase is the $AlCu_3$-based substable supersaturated solid solution. It has a space lattice structure of rhomboidal crystal system and good hardness and strength. Fe-containing hard K phase is a hard reinforcement phase and it has the characteristics of high melting points and high hardness. And its dispersion distribution can improve the comprehensive performance of the coating [0].

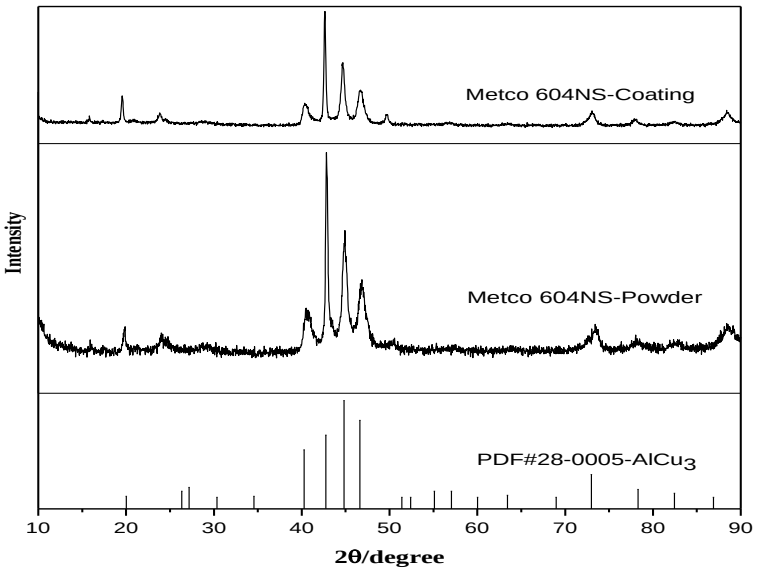

Fig. 11. XRD pattern of the aluminum bronze/polyester coating and powder.

Comparing the diffraction pattern of powder and coating, it can be seen that the basic compositions are basically the same before and after spraying, and the XRD diffraction peak of powder is higher than that of the coating, mainly because the sprayed particles hit on the surface of the matrix material at high speed, plastic deformation occurs, making the grain refinement, which leads to the coating diffraction peaks decrease in intensity.

3.4. Thermogravimetric differential thermal analysis

3.4.1. Metco 601NS

Figure 12 shows the TG-DTA curves of the AlSi-polyester powders in air. The nominal composition of Metco 601NS is Al7Si40polyester. The TG curve shows that from 485^{o}C to 670^{o}C the powders lose weight for 40%, which means the composite powders are stable below 485^{o}C and above 670^{o}C polyester will be burnt out totally. The exothermic peaks in the DTA curve at 565^{o}C and 630^{o}C are the results of the polyester degradation and oxidation of carbon from polyester. Above 670^{o}C, the powder weight increases due to oxidation of melted Al, Al-Si alloy and Si.

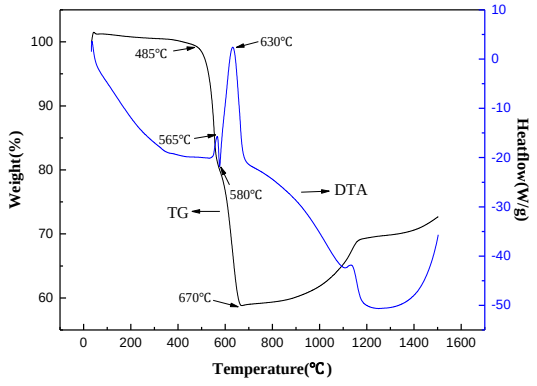

Fig. 12. TG-DTA curves of AlSi-polyester powders.

3.4.2. Metco 604NS

Figure 13 shows the TG-DTA curves of the aluminum/bronze polyester powders in air. The nominal composition of Metco 604NS is Cu8.5Al1Fe5polyester. The TG curve shows that from 478°C to 622°C the powders lose weight for 4%, which means the composite powders are stable below 478°C and above 622°C polyester will be burnt out totally. The exothermic peaks in the DTA curve at 543°C and 595°C are the results of the polyester degradation and oxidation of carbon from polyester. Above 622°C, the powder weight increases due to oxidation of melted Al, Cu and Fe and their alloys.

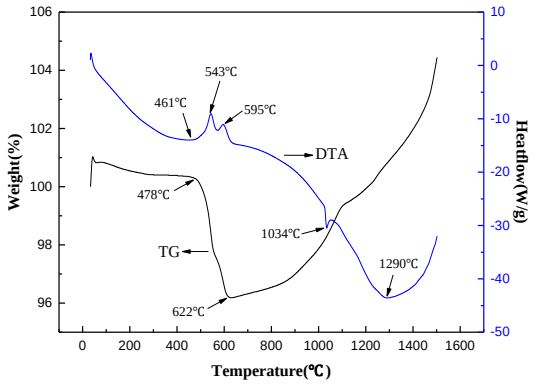

Fig. 13. TG-DTA curves of aluminum/bronze polyester powders.

The TG-DTA curves of Metco 601NS and Metco 604NS powders in air are similar. Because Metco 604NS powders only contain 5% polyesters, polyesters are burnt out below 622°C. For Metco 601NS powders, they contain 40% polyesters, polyesters are burnt out totally until 670°C and the two exothermic peaks intensities corresponding to polyester degradation and oxidation of carbon from polyester are higher than that of Metco 604NS, which means more heat are released due to more polyesters degradation and oxidation of carbon from polyester.

4. Conclusion

In summary, SEM, XRD and TG-DTA were performed to compare the reaction mechanism of AlSi-polyester and aluminum bronze/polyester. From the preparation of the powder and the process of coating, there are many similarities. For example, both use plasma spraying. The AlSi-polyester and aluminum bronze/polyester powders are prepared by blending method. Neither of the coating service temperatures exceed 500°C. The coatings are all mechanically bonded. The phases of the powder and coating are almost identical, the spraying process did not produce other compounds.

There are also many differences between them. For example, the bond coat is required before spraying the AlSi-polyester coating, while Metco 604NS powder can be directly sprayed on the substrate by APS. The TG-DTA curves of Metco 601NS and Metco 604NS powders are similar in air. However, due to the different proportion of polyester, there are some differences between the two powders. Coating prepared with Metco 604NS has lower porosity due to lower

polyester percentage (5%) and better melting effect of spherical aluminum bronze powders. Other properties such as hardness and abrasion resistance will be studied further.

Acknowledgements

The project was supported by “20 Policies about Colleges in Jinan” Program (Grant NO: 2019GXRC047), "migratory bird like" high level talent program in Tianqiao District and the provincial innovation and entrepreneurship training program of Qilu University of Technology (S202010431089).

References

[1] Y. Yue , Z. X. Zhao , G. Q. Lu et al., Thermal Spray Technology **6**(1), 40 (2014).
[2] L. Y. Chen, University of Science and Technology Beijing, (2018).
[3] L. Li, Z. Wei, M. Z. Yuan et al., NDT and E International **108**, 1 (2019).
[4] R. C. Bill, Ludwig. L. P, Wear **1**(59), 165 (1980).
[5] L. M. Chen, Q. Li, Heat Treatment Technology and Equipment **27**(1), 1 (2006).
[6] X. Ma, A. Matthews, Wear **9**(267), 1501 (2009).
[7] L. F. Tang, W. S. Li, L. He et al., The Chinese Journal of Nonferrous Metals **29**(5), 931 (2019).
[8] Y. J. Chen, Z. P. Wang, K. Y. Ding, Material Protection **43**(3), 7 (2010).
[9] J. W. Wu, J. G. Yang, H. Y. Fang et al., Applied Surface Science **22**(252), 7809 (2006).
[10] D. Jech, L. Čelko, P. Komarov et al., Solid State Phenomena **270**, 224 (2017).
[11] H. W. Zhang, B. H. Shi, X. D. Luo et al., Metallurgical Collections **4**, 4 (2015).
[12] C. Hu, ICIMM 2015, Taizhou University, (2015).
[13] Durairaj, R. B, Mageshwaran, G, Jeyajeevahan, J et al., Digest Journal of Nanomaterials and Biostructures **2**(14), 343 (2019).
[14] C. H. Ji, S. Zhang, X. Ma et al., Surface Technology **49**(2), 165 (2020).
[15] X. Y. Cheng, J. M. Liu, D. M. Zhang et al., Thermal Spray Technology **8**(1), 63 (2016).
[16] S. Wang, J. Yang, Z. Chang et al., Material Protection **51**(11), 57 (2018).
[17] A. S. Jabur, Powder Technology **237**, 477 (2013).
[18] J. Yang, Y. L. An, X. Q. Zhao et al., Journal of Materials Engineering **9**, 8 (2014).
[19] K. Murakami, N. Takuno, T. Okamoto et al., Materials Science and Engineering **1**(154), 93 (1992).
[20] T. T. Cheng, K. Y. Ding, C. H. Ji et al., Transactions of Materials and Heat Treatment **38**(9), 148 (2017).
[21] R. E. Johnston, Surface and Coatings Technology **10**(205), 3268 (2011).
[22] H. Liu , N. Tan, X. Y. Jin, Heat Treatment of Metals **44**(9), 147 (2019).
[23] S. Alam, S. Sasaki, H. Shimura, Wear **248**, 75 (2001).
[24] L. Z. Zhang, Shenyang University of Technology, (2007).